

Lee-Yang edge singularities in QCD: From Fourier coefficients to parametrizations of the universal scaling functions

Christian Schmidt^a

^a*Fakultät für Physik, Universität Bielefeld, Universitätsstraße 25, 33615 Bielefeld, Germany*

E-mail: schmidt@physik.uni-bielefeld.de

We will discuss the singular structure of the QCD phase diagram, present in the vicinity of the Roberge-Weiss and chiral phase transitions in QCD. We discuss two methods to extract complex singularities from lattice QCD observables calculated at imaginary baryon chemical potential, rational approximations and Fourier coefficients. We emphasize that the singularities in the complex chemical potential plane can be interpreted in terms of Lee-Yang edge singularities with known universal scaling behavior. Their universal scaling manifests as properties of the order parameter scaling function f_G . A particular parametrization of f_G based on Schofield is frequently used, is presented. We show that the parametrization also exhibits the universal position of the Lee-Yang edge. We emphasize that scaling fits to the Lee-Yang edge can be used to determine the (non-universal) location of phase transitions in QCD.

*European network for Particle physics, Lattice field theory and Extreme computing (EuroPLEx2023)
11-15 September 2023
Berlin, Germany*

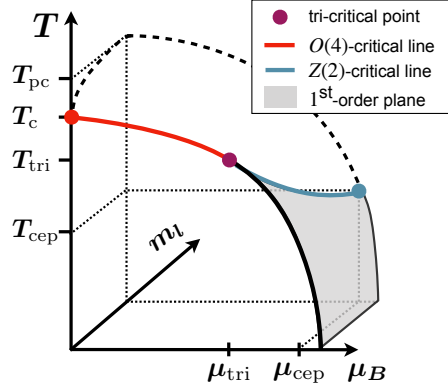


Figure 1: Schematic representation of the (2+1)-flavor QCD phase diagram. Solid lines represent 2^{nd} order phase transition lines and 1^{st} order critical surfaces. Where $O(4)$ and $Z(2)$ critical lines meet we have a tri-critical point. Dashed lines indicate pseudo-critical lines (crossover).

1. Introduction

Clarifying our knowledge on the QCD phase diagram is one of the outstanding and most pressing tasks in high energy physics. A detailed and quantitative understanding of the phase diagram in the temperature (T) and net baryon chemical potential (μ_B) plane is mandatory for cosmology, astro-physics and heavy ion phenomenology. While large scale experimental efforts are performed to investigate the phase diagram in heavy ion experiments (see e.g. [1]), direct first principle lattice QCD calculations are hindered by the infamous sign problem. We thus have to rely on indirect methods, which are based on the calculation of Taylor expansion coefficients of the partition function with respect to μ_B about zero ($\mu_B = 0$) [2] or imaginary ($\mu_B = i\theta_B$) [3]. Analytic continuations and extrapolations based on those expansion coefficients suffer from large statistical and systematical uncertainties [4]. Here we argue that the zeros of the partition function Z , i.e. poles of $\log Z$, are stable observables that can be used to locate phase transition points in QCD. Among these, the elusive QCD critical point is most important and its location is considered a grand challenge in lattice QCD.

The method relies on the identification of the closest singularity with the Lee-Yang edge (LYE). That such identification is sensible has been shown in the vicinity of the Roberge-Weiss transition in lattice QCD [5], as well as in the Ising model [6, 7]. In both cases known results are reproduced successfully and expected LYE scaling was observed. In detail, we trace the first singularity in the complex μ_B plane for a number of temperatures. We fit the positions to a universal scaling ansatz that can be used to extrapolate the LYE to the real domain, where it corresponds to a physical phase transition.

The application of the universal scaling ansatz depends on the mapping of the QCD parameters T , μ_B , m_l and m_s to the universal scaling fields of the universal model, denoted as reduced temperatures t and reduced symmetry breaking field h . In the following, we consider a situation with two degenerate light quarks and one heavier strange quark with masses m_l and m_s , respectively. Our current understanding of the (2+1)-flavor QCD phase diagram, where the strange quark mass m_s is kept fixed to its physical value, is summarized in Fig. 1. We see that we expect a second order

phase transition in the chiral limit ($m_l \rightarrow 0$) of QCD. It is commonly assumed that this transition is in the $O(4)$ symmetry class [8]. This transition extends towards $\mu_B > 0$ until it turns into a first order transition at a tri-critical point [9]. Starting from the tri-critical point we also expect a line of $Z(2)$ second order phase transitions extending towards $m_l > 0$. At physical quark masses this transition corresponds to the famous QCD critical point.

Not shown in Fig. 1 is the Roberge-Weiss (RW) transition [10], which is located at imaginary chemical potential $\mu_B = i\pi T$ and temperatures larger than the pseudo-critical temperature $T > T_{pc}$ [11, 12]. This phase transition is a remnant of the center symmetry of the gauge group and also belongs to the $Z(2)$ universality class. In the following, we consider three critical points in the QCD phase diagram where we map the QCD parameters to the universal scaling fields t, h , the RW transition, the chiral transition and the QCD critical point. At each of these points the symmetry breaking field is different and thus the mapping to QCD. We have [5, 13]

$$\begin{array}{lll}
 \text{RW transition:} & \text{chiral transition:} & \text{QCD critical point:} \\
 t = t_0 \left(\frac{T - T_{RW}}{T_{RW}} \right), & t = t_0 \left(\frac{T - T_c}{T_c} + \kappa_B^2 \hat{\mu}_B^2 \right), & t = \alpha_t (T - T_{cep}) + \beta_t (\mu_B - \mu_{cep}), \\
 h = h_0 \left(\frac{\hat{\mu}_B - i\pi}{i\pi} \right), & h = h_0 \left(\frac{m_l}{m_s} \right), & h = \alpha_h (T - T_{cep}) + \beta_h (\mu_B - \mu_{cep}).
 \end{array}$$

Here we define $\hat{\mu}_B = \mu_B/T$ and t_0, h_0 are non-universal normalization constants. Note that for the first two cases we have a good understanding of the symmetry breaking fields. In particular, for the chiral transition it is well known that the light quark mass m_l drives the symmetry breaking and that the chemical potential couples to the temperature like scaling field t with a coupling that is known to quite some precision [14, 15]. In the last case we assume the most general mapping [16], which is a linear mixing ansatz, which holds true in the immediate vicinity of the QCD critical point.

2. Lee-Yang zeros and edge singularity

Universal critical behavior is usually analyzed in terms of the (magnetic) equation of state. The singular part of the free energy is a generalized homogenous function of the scaling variables t, h . This leads to the fact that we can express the scaling function of the order parameter $M = \partial \ln Z / \partial h$ as function of a single scaling variable $z = t/h^{1/\beta\delta}$, where the critical exponents β, δ , determine the universality class. We have the relation

$$M = h^{1/\delta} f_G(z), \quad (1)$$

where $f_G(z)$ is the scaling function of the order parameter. An alternative approach to the universal behavior is provided by the zeros of the partition function in a finite volume V . In particular, the way how the zeros scale with the volume and under which angle they approach the real domain [17], gives information on the universality class and the location of the critical point. In Fig. 2 we indicate the schematic behavior of the Lee-Yang zeros. On the right, the situation in a finite volume is shown at a reduced temperature $t > 0$. The Lee-Yang theorem [18] predicts that all the zeros are located along the imaginary $h = \pm ih''$ axis. In the infinite volume limit, the zeros condense and form a branch cut (middle). The branch cut singularity is called the Lee-Yang edge

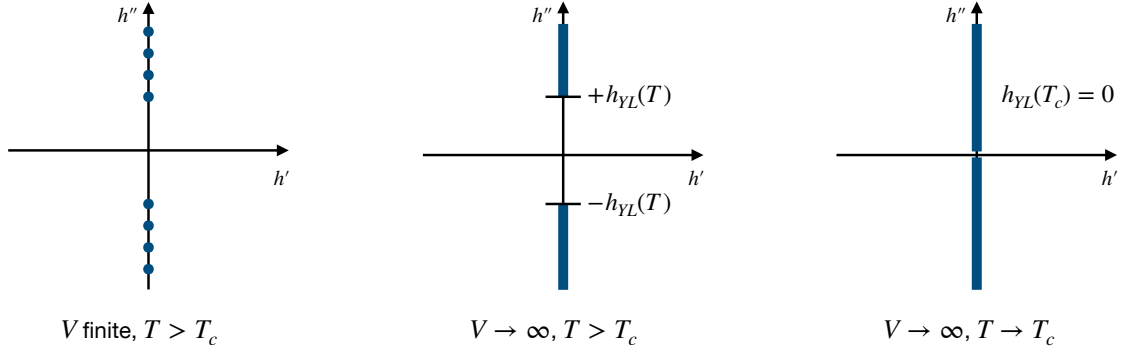


Figure 2: Schematic representation representation of Lee-Yang zeros in the complex $h = h' + ih''$ plane (left). The zeros accumulate to form a Lee-Yang cut if the thermodynamic limit ($V \rightarrow \infty$) is taken (middle). The onset of the cut is the Lee-Yang edge (LYE) singularity. The LYE pinches the real $h = h'$ axis for $T \rightarrow T_c$.

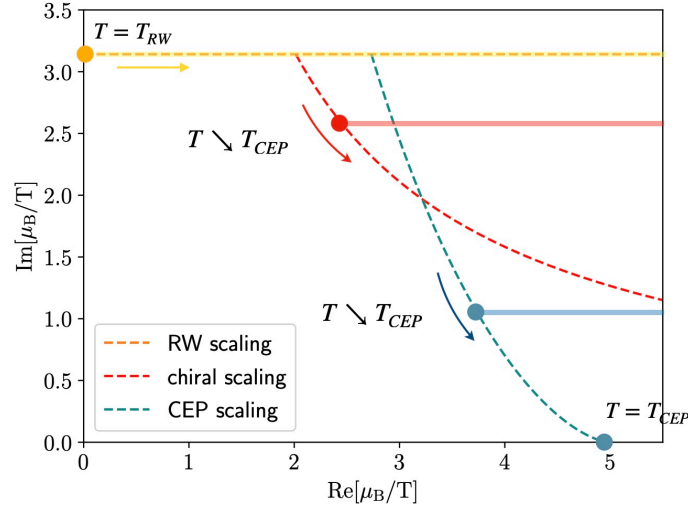


Figure 3: Schematic representation representation of the LYE scaling with temperature in the complex chemical potential plane.

(LYE). If the temperature is reduced to reach the critical point, the two branch cuts pinch the real domain (right). It is interesting to note that the Lee-Yang edge has a universal position in terms of the scaling variable z , we have $z_{LY} = |z_{LY}|e^{i\pi/(2\beta\delta)}$. The phase is a trivial consequence of the Lee-Yang theorem, the modulus z_{LY} has only been determined recently [19–22]. The fact that the LYE has a universal position $z = z_{LY}$, together with the above ansatz for the scaling variables t, h , is sufficient to picture the temperature scaling of the LYE in the complex chemical potential plane. A systematic illustration is given in Fig. 3. We expect that the LYE at $T = T_{RW}$ is located right at the RW transition ($\hat{\mu}_{LY} = i\pi$). For lower temperatures it becomes complex, first along the RW scaling line until it follows the chiral scaling line ($T \sim T_{pc}$). Finally it approaches the real axis for $T = T_{cep}$. Note that the CEP scaling line is not very well determined as normalization constants $\alpha_t, \alpha_h, \beta_t, \beta_h$ are unknown. The same is true for the critical temperature and chemical potential T_{cep} and μ_{cep} , even though first results have been obtained on cores lattices [23].

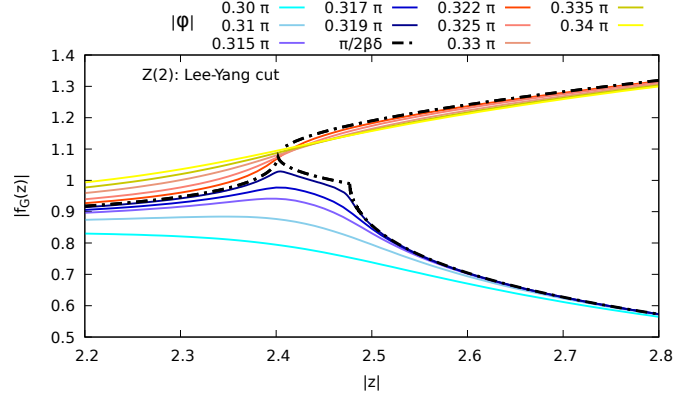


Figure 4: Lee-Yang cut in the scaling function $f_G(z)$. Shown is the absolute value $|f_G(z)|$ in the Schofield parametrization for different arguments of the complex scaling variable z as function of its modulus $|z|$. The figure is taken from Ref. [22]

The universal location of the LEY should also be encoded in the scaling function $f_G(z)$. The Schofield parametrization of the scaling function takes advantage of the asymptotic correct form for $z \rightarrow -\infty$ and the conventional normalization, i.e. $f_G(0) = 1$ and $f_G(z)/(-z)^\beta = 1$ for $z \rightarrow -\infty$ [24]. It introduces two alternative scaling variables R, θ in the form

$$t = R(1 - \theta^2) \quad \text{and} \quad h = h_0 R^{\beta\delta} h(\theta), \quad (2)$$

where the function $h(\theta)$ maps the entire complex z plane onto a compact region in θ . In particular, we have $z \rightarrow \infty$ for $\theta \rightarrow 0$, $z = 0$ for $\theta = 1$ and $z \rightarrow -\infty$ for $\theta \rightarrow \theta_0$. The Lee-Yang edge is located at the boundary of this region [22]. The entire non trivial information that defines the parameterization is encoded in the expansion coefficients of the function $h(\theta)$, which can be written as

$$h(\theta) = \theta \left(1 + h_3 \theta^2 + h_5 \theta^4 + \mathcal{O}(\theta^6) \right). \quad (3)$$

With these variables the scaling function is given as

$$f_G(z) = f_G(z(\theta)) = \theta \left(\frac{h(\theta)}{h(1)} \right)^{-1/\delta}. \quad (4)$$

The expansion coefficients h_3, h_5, \dots can be determined analytically, e.g. from ϵ -expansion [25, 26], but they can also be determined from Monte Carlo simulations [27]. It is interesting to note that the Lee-Yang cut imposes additional constraints on the expansion coefficients by the fact that the singularity is located at $\arg(z_{LY}) = \pi/(2\beta\delta)$ and additional singularities in $f'(z(\theta))$ have to line up along the cut [22]. In Fig. 4 we show the modulus of the scaling function $|f_G(z)|$ along lines of constant $\arg(z)$. The cut is seen at $\arg(z) = \pi/2\beta\delta$ as expected. We find the location of the singularity at $|z_{LY}| = 2.429(56)$ [22], which is in good agreement with the determination by means of the Functional Renormalization Group (FRG) [20, 21]. Note that the true edge exponent σ , i.e. the behavior $\Delta M \sim (h - h_{LY}(T))^\sigma$, is only restored in the limit of infinitely many expansion coefficients h_j .

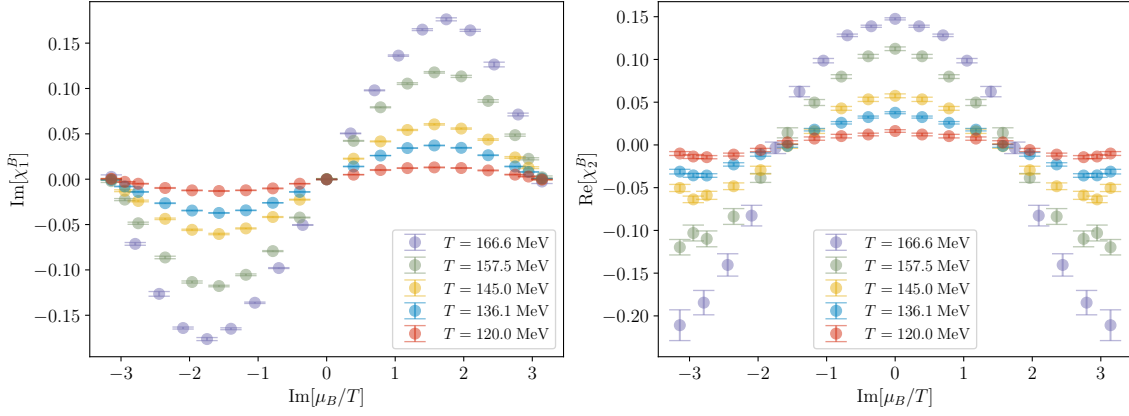


Figure 5: First (χ_1^B) and second (χ_2^B) cumulant of net baryon number as function of imaginary chemical potential for different temperatures. Data is obtained on $36^3 \times 6$ lattices [23]

3. Lattice setup and results

We perform lattice QCD calculations with (2+1)-flavor of highly improved staggered quarks (HISQ), using the SIMULATeQCD code [28]. Calculations at $\hat{\mu}_B > 0$ are unfeasible due to the infamous sign problem, we therefore perform a number of simulations at $\hat{\mu}_B = i\theta_B$, with $\theta_B \in [0, \pi]$. The observables we measure are the cumulants of the net baryon number, defined as

$$\chi_n^B(T, V, \mu_B) = \left(\frac{\partial}{\partial \hat{\mu}_B} \right)^n \frac{\ln Z(T, V, \mu_B)}{VT^3}. \quad (5)$$

Results from calculations on $36^3 \times 6$ lattices on χ_1^B and χ_2^B are shown in Fig. 5. The challenge now is to extract the Lee-Yang edge from this data. Since the data is periodic in θ_B with period 2π , it seems reasonable to analyze the data in terms of Fourier coefficients. As furthermore χ_1^B is an odd function of θ_B , it is natural to express χ_1^B by a Fourier sine form, defined by

$$\chi_1^B = \sum_{k=1}^{\infty} b_k(T) \sin(k\theta_B), \quad \text{with} \quad b_k(T) = \frac{2}{\pi} \int_0^{\pi} \chi_1^B(T, \theta_B) \sin(k\theta_B) d\theta_B. \quad (6)$$

The set of available Fourier coefficients $\{b_k(T)\}$ carry information on the baryon-baryon interaction, as the above Fourier expansion can be understood as a fugacity expansion [29]. In that spirit, $b_1(T)$ is just given by the partial pressure of the non-interacting baryon number $|B| = 1$ sector of the hadron resonance gas. The coefficient $b_2(T)$ parametrizes the leading order baryon-baryon interaction ($|B| = 2$). In their asymptotic behavior for $k \rightarrow \infty$, the information on the critical point is encoded [30, 31]. Deforming the integral in Eq. (6) into the complex plane, such that we integrate along the Lee-Yang cut, we can show that the Fourier coefficients behave as [31]

$$b_k = |\tilde{A}_{LY}| \frac{\exp\{-\hat{\mu}_{LY}^R k\}}{k^{1+\sigma}} \cos(\hat{\mu}_{LY}^I k + \phi_{LY}) + |\tilde{A}_{RW}| (-1)^k \frac{\exp\{-\hat{\mu}_{RW}^R k\}}{k^{1+\sigma}}, \quad (7)$$

where $\hat{\mu}_{LY}$ is the location of the LYE, associated with the chiral or CEP transition. Superscripts R, I refer to real and imaginary parts respectively. ϕ_{LY} refers to a nontrivial phase from the amplitude

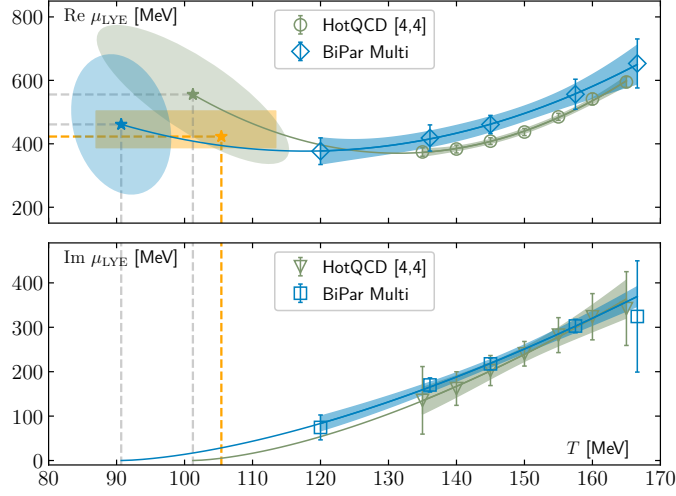


Figure 6: Scaling fits for the LYE singularities related to the CEP. Green data come from a [4,4] Padé from Ref. [32]. Blue data come from the multi-point Padé from Ref. [23]. Top: Scaling of the real part. Bottom: Scaling of the imaginary part. The ellipses shown in the top panel represent the 68% confidence region deduced from the covariance matrix of the fit. The orange box indicates the AIC weighted estimate [23].

A_{LY} . The last term explicitly lists the contribution from the RW transition which is located at $\mu_{RW}^I = \pi$, which turns the $\cos(\mu_{RW}^I k)$ into an alternating sign $(-1)^k$. This form can be used to predict the location of the LYE in the quark meson model [31]. Calculations in QCD are still work in progress as we require very precise numerical data to obtain conclusive results. In order to exploit not only the χ_1^B results in the numeric Fourier transform, but also the χ_2^B results, one can first perform a Hermité interpolation of the data, followed by an analytic evaluation of the Fourier integral. This is the strategy of a Filon-type quadrature on oscillatory integrals.

A further method to extract the LYE is based on a rational interpolation of the data, which can be obtained by multi-point Padé resummation. Unlike the standard Padé, the multi-point Padé is not very well known in literature but was exploited to extract Lee-Yang zeros in the vicinity of the RW transition [5] and in the Ising model [6, 7]. In these cases it was shown that the closest Lee-Yang zero indeed scales in accordance with the expected scaling of the LYE. The identification of the closest Lee-Yang zero with the LYE is thus justified. Some finite size effects, could however remain as it was pointed out recently [33]. In Fig. 6 we show the results on the LYE extracted by the multi-point Padé resummation in the vicinity of the CEP. The imaginary part of the the LYE position in the complex chemical potential plane is fitted with a power law, i.e. $\mu_{LY}^I \sim (T - T_{cep})^{\beta\delta}$, which is the leading order one obtains from the ansatz for the scaling variables t, h in the vicinity of the CEP together with the fact that the LYE has a constant location in the scaling variable $z = t/h^{\beta\delta}$. The real part is fitted with a second order polynomial ansatz. The results obtained yield a critical point at $(T_{cep}, \mu_{cep}) = (105_{-18}^{+8}, 422_{-35}^{+80})$ MeV [23]. Also shown are the results from the [4,4]-Pade resummation of the HotQCD Taylor expansion coefficients from $32^3 \times 8$ lattices [32], which yields a compatible but slightly higher result for $\mu_{cep} = 560(140)$ MeV, see also Ref. [34]. This is a hint on the size of the cutoff effects. However, many systematic effects need to be discussed in more detail in future, including lattice spacing and finite volume effects in the original data, as well as

systematics of the analysis as the dependence on the order of the Padé resummation.

Acknowledgments

CS acknowledges V. Skokov and all members of the HotQCD and Bielefeld-Parma Collaboration for valuable discussions. This work was supported (i) by the European Union’s Horizon 2020 research and innovation program under the Marie Skłodowska-Curie Grant Agreement No. H2020-MSCAITN-2018-813942 (EuroPLEx), (ii) by The Deutsche Forschungsgemeinschaft (DFG, German Research Foundation) - Project number 315477589-TRR 211 and the PUNCH4NFDI consortium supported by the Deutsche Forschungsgemeinschaft (DFG, German Research Foundation) with project number 460248186 (PUNCH4NFDI).

References

- [1] A. Bzdak, S. Esumi, V. Koch, J. Liao, M. Stephanov and N. Xu, *Phys. Rept.* **853** (2020), 1-87 [[arXiv:1906.00936 \[nucl-th\]](#)].
- [2] C. R. Allton, S. Ejiri, S. J. Hands, O. Kaczmarek, F. Karsch, E. Laermann and C. Schmidt, *Phys. Rev. D* **68** (2003), 014507 [[arXiv:hep-lat/0305007 \[hep-lat\]](#)].
- [3] M. D’Elia and M. P. Lombardo, *Phys. Rev. D* **67** (2003), 014505 [[arXiv:hep-lat/0209146 \[hep-lat\]](#)].
- [4] D. Bollweg *et al.* [HotQCD], *Phys. Rev. D* **108** (2023) no.1, 014510 [[arXiv:2212.09043 \[hep-lat\]](#)].
- [5] P. Dimopoulos, L. Dini, F. Di Renzo, J. Goswami, G. Nicotra, C. Schmidt, S. Singh, K. Zambello and F. Ziesché, *Phys. Rev. D* **105** (2022) no.3, 034513 [[arXiv:2110.15933 \[hep-lat\]](#)].
- [6] S. Singh, M. Cipressi and F. Di Renzo, *Phys. Rev. D* **109** (2024) no.7, 074505 [[arXiv:2312.03178 \[hep-lat\]](#)].
- [7] S. Singh, D. A. Clarke, P. Dimopoulos, F. Di Renzo, J. Goswami, F. Karsch, C. Schmidt and K. Zambello, *PoS EuroPLEx2023* (2024), 025
- [8] R. D. Pisarski and F. Wilczek, *Phys. Rev. D* **29** (1984), 338-341
- [9] M. A. Stephanov, K. Rajagopal and E. V. Shuryak, *Phys. Rev. Lett.* **81** (1998), 4816-4819 [[arXiv:hep-ph/9806219 \[hep-ph\]](#)].
- [10] A. Roberge and N. Weiss, *Nucl. Phys. B* **275** (1986), 734-745
- [11] C. Bonati, M. D’Elia, M. Mariti, M. Mesiti, F. Negro and F. Sanfilippo, *Phys. Rev. D* **93** (2016) no.7, 074504 [[arXiv:1602.01426 \[hep-lat\]](#)].
- [12] C. Schmidt, D. A. Clarke, P. Dimopoulos, F. Di Renzo, J. Goswami, S. Singh, V. V. Skokov and K. Zambello, *PoS LATTICE2023* (2024), 167 [[arXiv:2401.07790 \[hep-lat\]](#)].

- [13] C. Nonaka and M. Asakawa, *Phys. Rev. C* **71** (2005), 044904 [[arXiv:nucl-th/0410078 \[nucl-th\]](#)].
- [14] H. T. Ding, O. Kaczmarek, F. Karsch, P. Petreczky, M. Sarkar, C. Schmidt and S. Sharma, *Phys. Rev. D* **109** (2024) no.11, 114516 [[arXiv:2403.09390 \[hep-lat\]](#)].
- [15] S. Borsanyi, Z. Fodor, J. N. Guenther, R. Kara, S. D. Katz, P. Parotto, A. Pasztor, C. Ratti and K. K. Szabo, *Phys. Rev. Lett.* **125** (2020) no.5, 052001 [[arXiv:2002.02821 \[hep-lat\]](#)].
- [16] J. J. Rehr and N. D. Mermin, *Phys. Rev. A* **8** (1973), 472-480
- [17] C. Itzykson, R. B. Pearson and J. B. Zuber, *Nucl. Phys. B* **220** (1983), 415-433
- [18] C. N. Yang and T. D. Lee, *Phys. Rev.* **87** (1952), 404-409
- [19] A. Connelly, G. Johnson, F. Rennecke and V. Skokov, *Phys. Rev. Lett.* **125** (2020) no.19, 191602 [[arXiv:2006.12541 \[cond-mat.stat-mech\]](#)].
- [20] G. Johnson, F. Rennecke and V. V. Skokov, *Phys. Rev. D* **107** (2023) no.11, 116013 [[arXiv:2211.00710 \[hep-ph\]](#)].
- [21] V. Skokov, *PoS EuroPLEx2023* (2024), 026
- [22] F. Karsch, C. Schmidt and S. Singh, *Phys. Rev. D* **109** (2024) no.1, 014508 [[arXiv:2311.13530 \[hep-lat\]](#)].
- [23] D. A. Clarke, P. Dimopoulos, F. Di Renzo, J. Goswami, C. Schmidt, S. Singh and K. Zambello, “Searching for the QCD critical endpoint using multi-point Padé approximations,” [[arXiv:2405.10196 \[hep-lat\]](#)].
- [24] P. Schofield, *Phys. Rev. Lett.* **22** (1969), 606-608
- [25] R. Guida and J. Zinn-Justin, *Nucl. Phys. B* **489** (1997), 626-652 [[arXiv:hep-th/9610223 \[hep-th\]](#)].
- [26] M. Campostrini, M. Hasenbusch, A. Pelissetto, P. Rossi and E. Vicari, *Phys. Rev. B* **63** (2001), 214503 [[arXiv:cond-mat/0010360 \[cond-mat\]](#)].
- [27] F. Karsch, M. Neumann and M. Sarkar, *Phys. Rev. D* **108** (2023) no.1, 014505 [[arXiv:2304.01710 \[hep-lat\]](#)].
- [28] L. Mazur *et al.* [HotQCD], *Comput. Phys. Commun.* **300** (2024), 109164 [[arXiv:2306.01098 \[hep-lat\]](#)].
- [29] V. Vovchenko, J. Steinheimer, O. Philipsen and H. Stoecker, *Phys. Rev. D* **97** (2018) no.11, 114030 [[arXiv:1711.01261 \[hep-ph\]](#)].
- [30] G. A. Almási, B. Friman, K. Morita and K. Redlich, *Phys. Lett. B* **793** (2019), 19-25 [[arXiv:1902.05457 \[hep-ph\]](#)].

- [31] M. Bryant, C. Schmidt and V. V. Skokov, *Phys. Rev. D* **109** (2024) no.7, 076021 [[arXiv:2401.06489 \[hep-ph\]](#)].
- [32] D. Bollweg *et al.* [HotQCD], *Phys. Rev. D* **105** (2022) no.7, 074511 [[arXiv:2202.09184 \[hep-lat\]](#)].
- [33] T. Wada, M. Kitazawa and K. Kanaya, “Lee-Yang-zero ratios for locating a critical point,” [[arXiv:2410.19345 \[hep-lat\]](#)].
- [34] G. Basar, *Phys. Rev. C* **110** (2024) no.1, 015203 [[arXiv:2312.06952 \[hep-th\]](#)].